THE ASTROPHYSICAL JOURNAL, 485:328–332, 1997 August 10

INTERFEROMETRIC ANGULAR DIAMETERS OF MIRA VARIABLES WITH THE *HUBBLE SPACE TELESCOPE*[1]

MARIO G. LATTANZI,[2] ULISSE MUNARI,[3] PATRICIA A. WHITELOCK,[4] AND MICHAEL W. FEAST[5]
Received 1996 September 24; accepted 1997 March 11

ABSTRACT

This paper presents the first successful interferometric observations of angular diameters with the astrometer Fine Guidance Sensor (FGS) aboard the *Hubble Space Telescope*, the only optical interferometer operating in space. We report single-epoch angular diameters in visible light for the two Mira-type variables, R Leonis and W Hydrae, along two orthogonal directions. Although the relatively large bandpass of the instrument will limit the use of the new diameters for improving on our knowledge of the atmospheric structure of Mira variables, the milliarcsecond precision of the FGS measurements show with unprecedented clarity that the atmospheres of the two stars do not have circular symmetry, with the "major" axis exceeding the "minor" axis by about 11% and 20% for R Leo and W Hya, respectively. There is also evidence of nonsymmetric brightness distributions over the stellar disks. Besides the intrinsic interest of these results, asymmetries measured in a wide optical band, such as that used in the present work, are of relevance for the interpretation of the HIPPARCOS astrometry of Mira variables.

Subject headings: stars: fundamental parameters — stars: individual (R Leonis, W Hydrae) — stars: oscillations — stars: variables: other — techniques: interferometric

1. INTRODUCTION

The interferometric (TRANS) mode of the astrometer Fine Guidance Sensor (FGS) on the *Hubble Space Telescope* (*HST*) is currently used for a variety of research projects. Observing programs on a number of astrophysically important double stars (orbital and spectroscopic binaries with early- or late-type primaries, low mass binaries, etc.) were initiated soon after the launch of the *HST* (Franz et al. 1991, 1992; Bernacca et al. 1993, 1995). More recently, attempts toward a better understanding of the potential range of astrophysical applications of the FGS have demonstrated that the device can perform at its best (i.e., $\sim$10 ms of arc [mas] angular resolution in visible light) on more complex sources, such as the relatively crowded Large Magellanic Cloud (LMC) clusters embedded in strong diffuse backgrounds (Lattanzi et al. 1994 and references therein). Resolving stellar discs seemed likely to be the next very rewarding research field the FGS could profitably tackle, and this paper reports on the first direct angular diameter measurements in visible light with the *HST*.

Mira-type variables occupy a position at the tip of the asymptotic giant branch (AGB) of about 1 $M_\odot$ stars. They lose mass at a relatively high rate (from about 10^{-7} to 10^{-6} $M_\odot$ yr^{-1} to, in extreme cases, about 10^{-4} $M_\odot$ yr^{-1}) and are the last AGB stage before the objects evolve rapidly into planetary nebulae (see, e.g., Feast & Whitelock 1987 for a review). During their variability cycle, which is between about 100 and 500 days (at least for optically selected Mira variables), these stars undergo large amplitude light changes of $\Delta V \gtrsim 2.5$ mag. Mira-type variability is believed to be due to pulsation, although the pulsation mode remains uncertain.

Ground-based high-resolution interferometric techniques such as speckle interferometry, nonredundant masking, and Michelson interferometry have found evidence of asymmetries in *o* Ceti (Mira) (Karovska et al. 1991; Quirrenbach et al. 1992; Haniff et al. 1992) and in R Leonis (Tuthill et al. 1994). There are a number of possible explanations for such asymmetries. These include nonradial pulsation, rotational distortion of the outer envelope, and large spots on the stellar surface (possibly a manifestation of giant convection cells).

The determination of the sizes and shapes of Mira variables and the variation of these quantities with time is of fundamental importance for our understanding of the atmospheric structure, mass-loss, evolution, and pulsational properties of these stars. In addition, a better understanding of the outer regions of Mira variables is of importance for understanding the observed period luminosity (PL) relation for this class of variable (Feast et al. 1989). The PL relation is believed to have the same zero point in the LMC as in the Galaxy (Whitelock et al. 1994), suggesting that the relation is universal and making these stars important galactic and extragalactic distance indicators (Whitelock & Catchpole 1992).

In this work we concentrate on the first derivation of new high signal-to-noise (S/N) ratio angular sizes with the astrometer FGS aboard the *HST*. We also discuss (§ 4) preliminary comparisons with the most recent ground-based determinations, including considerations on the complex structure of the atmosphere of these stars and the wide filter bandpass of the FGS observations. More detailed consideration on the impact of these measurements on the physics of the two pulsating giants R Leonis and W Hydrae, and of Mira-type stars in general, has to await for further investigations and the completion of our *HST* program, which aims at measuring size and shape of these two Mira variables over a complete variability cycle.

[1] Based on observations with the NASA/ESA *Hubble Space Telescope*, obtained at the Space Telescope Science Institute, which is operated by AURA, Inc., under NASA contract NAS 5-26555.

[2] Osservatorio Astronomico di Torino, Strada Osservatorio 20, 10025 Pino Torinese TO, Italy. Also, Space Telescope Science Institute.

[3] Osservatorio Astronomico di Padova, Sede di Asiago, I-36132 Asiago (VI), Italy.

[4] South African Astronomical Observatory, P.O. Box 9, Observatory, 7935, South Africa.

[5] Astronomy Department, University of Cape Town, Rondebosch, 7700, South Africa.

TABLE 1

OBSERVING LOG

Parameter	R Leo	W Hya
UT Start of Observation.....	1995 Nov 6 22:08:55	1995 Dec 17 22:48:13
Duration (s)[a]	2289	2288
Filter ($\lambda/\Delta\lambda$, nm)	583/234[b]	583/234
Scan length	1.″5/axis	1.″5/axis
Number of scans.....	30	30
Scan orientation[c]	65.°6	53.°4
Variability phase.....	0.71	0.51
Pulsation period (day).....	312	373

NOTE.—The variability phases have been calculated using recent AAVSO data.

[a] This includes overheads. Actual usable time was 1875 s for both targets.

[b] Bandpass refers to the FGS unit as a whole (relay optics and photomultiplier tubes).

[c] See § 2.1 for an explanation.

2. OBSERVATIONS

The Mira-type stars selected for our interferometric study with the astrometer FGS are the two M8e giants R Leonis (HD 84748, IRAS 09448+1139) and W Hydrae (HD 120285, IRAS 13462−2807).[6] The journal of observations is given in Table 1.

The observations were made using the interferometric mode (TRANS mode) of the astrometer FGS (FGS3) (Holfeltz et al. 1995). In this mode of operation, the interferometer response function (RF) (or visibility fringe) is produced by moving the instantaneous field of view of the FGS across a star, i.e., by constantly changing the inclination of the compressed afocal beam from the primary mirror at the entrance face of the Koester's prism, the core optical element of the interferometer. High S/N ratio RFs are discussed in § 2.2 below; however, it is worth mentioning here that the approximate extension of an RF from (positive) peak–to–(negative) peak is ≈40 mas for unresolved stars, as shown in the top two panels of Figure 1 (Bradley et al. 1991; see also Benedict et al. 1992 and the works quoted in Lattanzi et al. 1994 for in-flight performances).

The FGS has two such interferometric units. These units, thanks to a polarizing beam splitter before the two Koester's prisms, provide RFs, $S(x)$ and $S(y)$, in two orthogonal directions, referred to as the X and Y axes in detector space. Each TRANS scan is always at 45° to the X-axis; therefore, the actual scan length (as projected on the sky) is $2^{1/2}$ times that on each axis.

2.1. *Interferometric Scans*

Each scan through either of the two targets was 1.″7 long, which gives a 1.″5 projected length on each axis. Thirty consecutive scans were taken during each observation. FGS3 was commanded to accomplish each scan in steps (pixels) of 0.6 mas, with the integration time set to the default value of 0.025 s pixel^{-1}. Such fine bins allow oversampling of the interferometer RF while still providing adequate S/N ratio per resolution element.

[6] W Hya is sometimes classed as an SRa-type variable because the amplitude and shape of its light curve can vary from cycle to cycle. However, it has a photographic light amplitude of about 4 mag, has typical Mira-type atomic emission lines in its optical spectrum, and is an OH, H_2O, and SiO maser. It appears therefore to belong physically with the Mira variables.

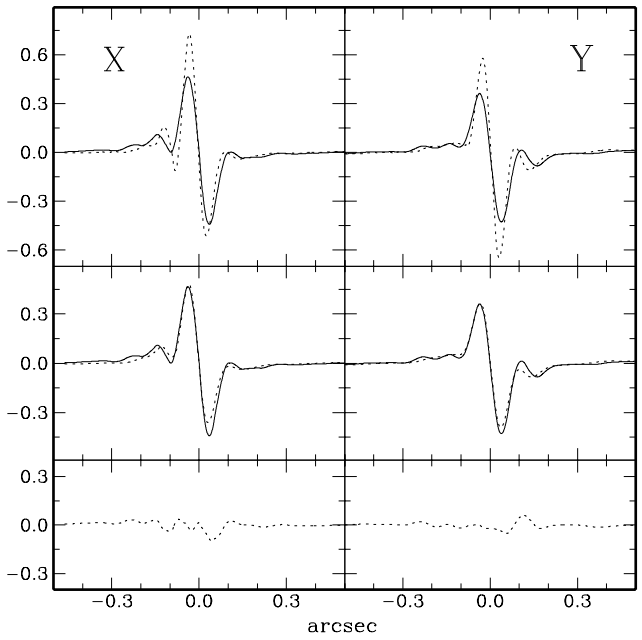

FIG. 1.—Interferometric measurement of R Leo. The solid lines represent the *observed* RFs on the two FGS axes. The top panels show the best possible overlap between observed and (unaltered) template RFs (*dotted lines*). The plots in the middle panels depict the resulting best-fit synthetic RFs (*dotted lines*) superposed to the observed ones. Graphs of the residuals of the difference best fit minus observed RFs are shown in the bottom panels.

Among the very limited selection of filters available with the FGS, we decided to use the PUPIL element. This is a 1/3 field stop, which therefore reduces by the same amount the effective diameter of the *HST* primary mirror "seen" by the interferometer. This is useful because the spherical aberration of the primary mirror, which has not been corrected by COSTAR in the external region of the telescope field of view used by the FGS, compounded with known FGS misalignments reduces the visibility of the RF and adds spurious structures to it. Thus, by using the PUPIL element, the most aberrated portions of the incoming beam are blocked out, partially restoring the visibility and shape of the theoretical RF. Experience has shown that optimal sensitivity is achieved with the PUPIL filter, especially on the more complex targets (Lattanzi et al. 1994).

The on-sky orientations of the interferometric scans are defined as the astronomical position angle (P.A.) of the negative direction of the X-axis and can be recovered from the spacecraft attitude parameters provided with the science data. They were 65.°6 and 53.°4 for R Leo and W Hya, respectively.

As shown in Lattanzi et al. (1994), the (instrumental) effective wavelength and system bandpass of the FGS when used in combination with the PUPIL filter are approximately 583 nm and 234 nm, respectively (see § 4 for considerations related to the effective wavelength of the system after convolution with the energy distribution of our targets).

2.2. *Error Sources*

There are two main reasons for taking multiple consecutive scans through the targets: (1) improving the S/N ratio of the fringes, and (2) detecting anomalous spacecraft jitter, i.e., sudden changes in the telescope line of sight while per-

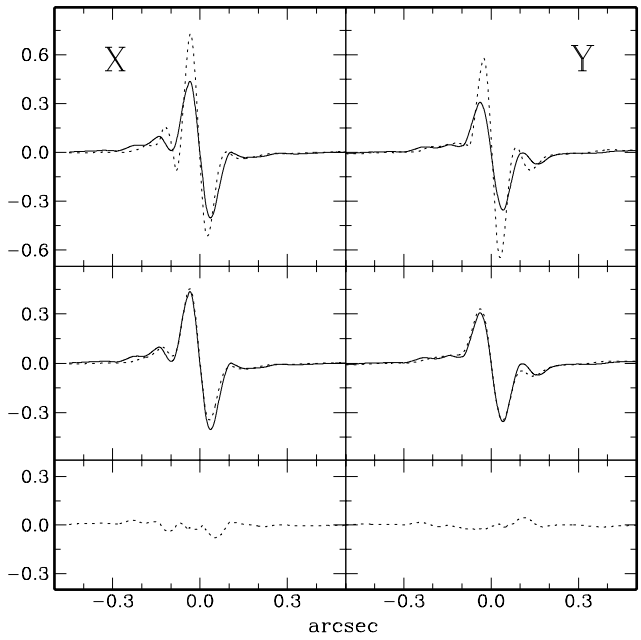

FIG. 2.—Interferometric measurement of W Hya. Plots are the same as in Fig. 1.

forming scans. The S/N ratio of individual RFs can be improved by stacking the output of $N_{\rm scan}$ consecutive scans, after allowing for possible scan-to-scan offsets. Under normal conditions this process results in merged RFs with S/N ratios about $(N_{\rm scan})^{1/2}$ times better than the initial ones (Lattanzi et al. 1994; Holfeltz & Lattanzi 1997). The effects of "guiding" errors of the kind mentioned in (2) would show up as artifacts in the shape of the normalized visibility fringe. Detection of such artifacts usually results in the rejection of the particular scan; smaller artifacts, which go undetected, will add to the final error budget in a way that could systematically alter the results. In practice, only those scans taken in normal jitter ($\sim$2 mas rms; see Bradley et al. 1991) are merged and used in the measurements. Because of the $(N_{\rm scan})^{1/2}$ law, this does not usually have any drastic impact on the S/N ratio of the merged scan. Three of the 30 scans secured on R Leo and two of the 30 on W Hya were rejected because of detected anomalies in the RFs. The measured S/N ratio per scan is about 100, and that of any of the four merged scans is about 500. Such large S/N ratios imply that the actual (merged) RFs are indistinguishable from their least-squares fits shown as solid lines in the top panels of Figures 1 and 2.

As expected, both $S(x)$ and $S(y)$ change with the color of observed objects; in particular, their main and secondary lobes appear stretched at longer effective wavelengths, i.e., for redder objects. For accurate results, it is therefore crucial to use those calibration (single) stars that match, as closely as possible, the color of the targets (Holfeltz & Lattanzi 1997). In addition, the angular scale along the interferometer axes could change with time, thus mimicking the color effect. Thus, for best results, calibration star data should also be obtained as close in time as possible to the actual observations.

3. MEASUREMENTS

The method of analysis is similar to the trial-and-error procedure described in Bucciarelli et al. (1992), which was originally devised for the interpretation of double star interferograms. In the present case, the observed RFs are cross-correlated with synthetic ones derived from stellar disc models.

3.1. *Synthetic Response Function for Resolved Stars*

A model for the synthetic X-axis RF of a resolved star can be inferred by following the arguments given in Lattanzi et al. (1995) for the multiple-star model and extrapolating them to the "continuous" case. For a circular disk one has

$$C(x,\rho)=\frac{\int_{-\rho}^{+\rho}\left[\int_0^{\rho\sin\theta(r)}B(\eta,r)d\eta\right]T(x-r)dr}{\int_{-\rho}^{+\rho}\left[\int_0^{\rho\sin\theta(r)}B(\eta,r)d\eta\right]dr}, \quad (1)$$

where ρ is the radius of the stellar disk, $\sin\theta(r)=\sin[\cos^{-1}(r/\rho)]$, and $T(x-r)$ is the single-star RF (the so-called reference template) displaced along the X-axis by r. A similar equation holds for the Y-axis RF. The function $T(x-r)$ in equation (1) clearly shows how crucial the choice of the proper standard star is in constructing the best possible synthetic model for cross-correlation with the observed RFs. In particular, it is critical to select a template that best matches the color of the targets. Therefore, we used the template indicated in Table 2 ($B-V=1.9$), which is the one, among the standard stars made available by the Space Telescope Science Institute (STScI), with the most favorable combination of filter and color.

The function $B(\eta, r)$ represents the stellar surface brightness, which, in the circular approximation, is a function of distance from the disk center $d=(\eta^2+r^2)^{1/2}$. In the uniform disk (UD) approximation, i.e., $B(\eta, r)=$ const, equation (1) reads

$$\mathrm{UD}(x,\rho)=\frac{2}{\rho\pi}\int_{-\rho}^{+\rho}\sin\left[\cos^{-1}\left(\frac{r}{\rho}\right)\right]T(x-r)dr, \quad (2)$$

which is the model we have utilized for R Leo and W Hya.

3.2. *Results*

The UD model in equation (2) depends only on the angular diameter 2ρ. We then explored the interval $2\rho=[0\text{–}120]$ mas in steps of 2 mas in search of the best possible correlation between observed and synthetic RFs. Sharp correlation maxima were found for the values given in Table 2. The best-correlation results are illustrated in Figures 1 and 2.

TABLE 2

RESULTS OF FGS INTERFEROMETRIC MEASUREMENTS IN UD APPROXIMATION

Parameter	R Leo	W Hya
$X_{\rm axis}$ diameter (mas)	70 ± 2	76 ± 2
$Y_{\rm axis}$ diameter (mas)	78 ± 2	91 ± 2
Axial ratio	0.90	0.86
Position angle of "major" axis	155°.6	143°.4
Used scans	27	28
Template	LatCol1a[a]	LatCol1a

NOTE.—The entries *Axial ratio* and *Position angle of "major" axis* both assume that (1) the observed shape is elliptical and (2) the actual major axis is aligned with the on-sky orientation of the FGS axis, which resolved the *larger* diameter. The P.A. of the true major axis *cannot* be recovered with only two interferometric scans, and the quoted axial ratios are upper limits to the actual ones.

[a] $V=9.7$, $B-V=1.9$ (Holfeltz & Lattanzi 1997).

The internal consistency of our measurements was assessed by dividing the individual scans into two groups, one containing the odd scans and the other the even scans. The two sets were integrated into odd and even merged RFs, and the best-correlation procedure was independently rerun on them with the same step of 2 mas on the unknown diameters. The best-correlation values derived from these two sets were identical for both targets. These results indicate that, because of the very high S/N ratios of the target scans (and of those of the template), the combined contribution of the observing errors to the final angular diameter estimates is smaller than the numerical resolution of the best-correlation procedure utilized (see Bernacca et al. 1993 for a similar discussion). Therefore, a conservative estimate on the measurement precision (in the UD approximation) can be set to 2 mas, i.e., the size of the step utilized to explore the adopted range of angular diameter values.

The external accuracy is difficult to estimate. As described earlier, target-template color mismatches, scale-like changes with time, and undetected anomalous jitter events all contribute to increasing the external error budget. Actual estimates might become available as data on our template are accumulated over the next *HST* cycles as a result of the routine calibration programs run by the STScI in Baltimore.

Given the extremely high S/N ratios reached in our observations, the "residual" differences between the observed RFs and the best-fit UD models, plotted in the bottom panels of Figures 1 and 2, appear as real and should be interpreted as unmodeled atmospheric effects to be included in a more realistic (and complex) version of the brightness function B. Work on Gaussian stellar disks, limb-darkening effects, and possible asymmetries in the disk shapes is in progress.

4. DISCUSSION

The atmospheres of Mira variables are very deep, and the effective diameters of the stars change markedly with wavelength, mainly because of the opacity effects of the TiO absorption bands (e.g., Labeyrie et al. 1977). Our UD diameters average over the wide bandpass of our filter (from $\sim$460 to $\sim$700 nm), although they will obviously be weighted to regions of greater flux, i.e., to longer wavelengths and outside the strongest TiO absorption bands. In other words, ignoring for the moment instrumental effects (e.g., the detailed transmission function of the instrument), a convenient expression for the FGS UD diameters, $R_{\rm FGS}$, as a function of the uniform-disk diameters, $R(\lambda)$, measured at other wavelengths, λ, is given by

$$R_{\rm FGS} \sim \frac{\int_{\lambda_1}^{\lambda_2} F(\lambda)R(\lambda)d\lambda}{\int_{\lambda_1}^{\lambda_2} F(\lambda)d\lambda},$$

where $\lambda_1 \sim 460$ nm and $\lambda_2 \sim 700$ nm represent the wavelength limits of the spectral response of the FGS setup used in our observations, and $F(\lambda)$ is the measured flux at the given λ. We notice that the TiO molecular band at 710 nm is mostly outside the bandpass of our observations. Also, the flux over the FGS spectral range changes typically by more than a factor of about 25, going from about 460 nm longward, with the peak at 700 nm.

In the case of R Leo, the angular diameters reported in Di Giacomo et al. (1991) and by Haniff, Scholz, & Tuthill (1995) in regions within the FGS bandpass support the rough approximation that $R_{\rm FGS} \sim R(700\ {\rm nm})$. This occurs because $F(\lambda)/F(700\ {\rm nm})$ is always less than 1, and $R(\lambda)$ is such that the ratio $[F(\lambda)R(\lambda)]/[F(700\ {\rm nm})R(700\ {\rm nm})]$ is significantly smaller than 1 at all relevant wavelengths. Considerations similar to these should be applicable to the measurements of W Hya. Therefore, if we can interpret the $R(\lambda)$ values as stratification of the extended atmospheres, then the FGS diameters trace mainly the atmospheric region contributing to the 700 nm continuum window. Emissions from outer layers manifest themselves as relatively small biases of the order of a few milliarcseconds.

Averaging our results over the two directions and comparing them to the latest measurements of Haniff et al. (1995) yields differences (in the sense FGS minus ground-based) of approximately 10 ± 6 mas and 19 ± 6 mas for R Leo and W Hya, respectively. Although caution is in order when discussing the accuracy (as opposed to precision) of our measurements (see § 2), the FGS diameter of R Leo appears consistent, in the sense discussed in the previous paragraph, with the ground-based value.[7] The difference for W Hya appears significant, i.e., larger than the expected bandpass-related correction. However, the ground-based diameter was obtained near maximum light, whereas the *HST* value refers to a phase near visual light minimum; the measured difference could, therefore, be an indication of increased dimensions (at least, of the particular atmospheric layer traced with the FGS) at visual light minimum.

Detailed comparisons are awaiting further modeling[8] and the results of our *HST* monitoring program, which should indicate the extent to which the diameters of these Mira variables vary with phase.

Perhaps the most important result of these initial *HST* observations is the clear detection of deviations from circular symmetry in the resolved discs of both variables. A reconstructed image of R Leo at 800 nm, using non-redundant mask interferometry, was reported in Tuthill et al. (1994), but no estimation of the axial ratio is attempted in that paper. The contour levels representing the two-dimensional image of R Leo (see their Fig. 1*a*) do show hints of ellipticity, which are consistent with our axial ratio of about 90%, although the P.A. of their major axis appears roughly orthogonal to that of our larger diameter. This difference might be another example of the changes in orientation of asymmetry with wavelength noticed by Karovska et al. (1991) in *o* Cet, although the measurements of Tuthill et al. (1994) were close to the resolution limit of their instrumentation. Irrespective of whether or not asymmetries change with wavelength, it is useful to mention here the expected modest effect of the FGS large bandpass on the measured asymmetries. Indeed, substantial perturbations, of say 20% of the one-dimensional diameter at 700 nm (which does not seem to be our case, as discussed earlier), would reduce (or increase, depending upon the actual geometry of the perturbing layers) the measured asym-

[7] The variability phase of our R Leo observation, 0.71, is close to that of Haniff et al. (1995), 0.88. However, sensible variations from variability cycle to cycle in the measured diameters at a given phase have been reported (Karovska et al. 1991).

[8] This should include a more accurate definition of the FGS bandpass and the use of modern model atmospheres of Mira variables. These models, through the definition of the relative dimensions of the different emitting layers and their contribution to the total flux, will provide the means to quantify on an individual basis the accuracy of the approximation $R_{\rm FGS} \sim R\,(700\ {\rm nm})$.

metries by no more than about 2%. The asymmetry of W Hya is given here for the first time. The degree of ellipticity is more accentuated than for R Leo and closer to the values measured for *o* Cet (Karovska et al. 1991; Haniff et al. 1992; Quirrenbach et al. 1992). In the case of *o* Cet there might be some concern that the shape of the Mira was affected by its companion, which is close enough to be heated by the wind from the Mira (Deutsch 1958; Walker 1957; Warner 1972). Neither R Leo nor W Hya show evidence of interacting companions. It should also be noted that, since the *HST* scans are not necessarily aligned with the largest and smallest diameters of the stars, the quoted ellipticities are *minimum* values.

From the considerations above, it appears that the FGS, because of its large bandpass, is not in a position to provide more insight into the atmospheric structure of Mira-type variables. On the other hand, its very high sensitivity[9] is extremely useful in monitoring the evolution of asymmetries as a function of variability phase. This is certainly among the crucial observations that must be made in order to unravel the problem of pulsation in Mira variables. In particular, the FGS, through observations over a few pulsation cycles, could establish whether or not there exists a preferred orientation of the asymmetry. This should provide useful constraints on possible scenarios for the asymmetry.

Finally, the question of asymmetries in Mira variables and other very cool stars as measured in a wide optical band is quite important for the interpretation of the positions, proper motions, and trigonometric parallaxes that have been measured (in a broad optical band) for many of these stars with HIPPARCOS. The sizes of nearby Mira variables are 2 orders of magnitude greater than the errors of at least some of the HIPPARCOS measures. Asymmetries (especially if variable) may significantly affect these derived quantities.

We thank J. A. Mattei, director of the American Association of Variable Stars Observers (AAVSO), for providing us with recent, unpublished, visual photometric data of R Leo and W Hya. Use of the SIMBAD database (Strasbourg, France) is also acknowledged. We wish to thank also F. Guglielmetti for her assistance with the data reductions, and S. T. Holfeltz for help with data retrieval and development of computer code.

[9] As demonstrated by the very high S/N ratios achieved in our measurements.

REFERENCES

Benedict, G. F., et al. 1992, PASP, 104, 958
Bernacca, P. L., et al. 1993, A&A, 278, L47
———. 1995, A&A, 299, 933
Bradley. A., et al. 1991, PASP, 103, 317
Bucciarelli, B., et al. 1992, in Proc. Workshop The First Year of *HST* Observations, ed. A. L. Kinney & J. C. Blades (Baltimore: STScI), 238
Deutsch, A. J. 1958, AJ, 63, 49
Di Giacomo, A., et al. 1991, A&A, 249, 379
Feast, M. W., et al. 1989, MNRAS, 241, 375
Feast, M. W., & Whitelock, P. A. 1987, in Late Stages of Stellar Evolution, ed. S. Kwok & S. R. Pottasch (Dordrecht: Reidel), 33
Franz, O. G., et al. 1991, ApJ, 377, L17
———. 1992, AJ, 103, 92
Haniff, C. A., et al. 1992, AJ, 103, 1662
Haniff, C. A., Scholz, M., & Tuthill, P. G. 1995, MNRAS, 276, 640
Holfeltz, S. T., & Lattanzi, M. G. 1997, in preparation
Holfeltz, S. T., et al. 1995, Fine Guidance Sensors Instrument Handbook, Version 5.0 (Baltimore: STScI)
Karovska, M., et al. 1991, ApJ, 374, L51
Labeyrie, A., et al. 1977, ApJ, 218, L75
Lattanzi, M. G., et al. 1995, in IAU Symp. 166, Astronomical and Astrophysical Objectives of Submilliarcsecond Optical Astrometry, ed. E. Høg & K. Seidelmann (Dordrecht: Kluwer), 95
———. 1994, ApJ, 427, L21
Quirrenbach, A., et al. 1992, A&A, 259, L19
Tuthill, P. G., et al. 1994, MNRAS, 266, 745
Walker, M. F. 1957, in IAU Symp. 3, Nonstable Stars, ed. G. H. Herbig (Cambridge: Cambridge Univ. Press), 47
Warner, B. 1972, MNRAS, 159, 95
Whitelock, P. A., & Catchpole, R. 1992, in The Center, Bulge, and Disk of the Milky Way, ed. L. Blitz (Dordrecht: Kluwer), 103
Whitelock, P. A., et al. 1994, MNRAS, 267, 711